



Communication

Fast-response fluorescent probe with favorable water solubility for highly sensitive imaging of endogenous tyrosinase in living cells and zebrafish model

Zheng Li^a, Xiaofeng Xia^a, Yu You^a, Cuifen Lu^{a,*}, Guichun Yang^a, Chao Ma^a, Junqi Nie^a, Qi Sun^{b,*}, Shuilin Wu^a, Jun Ren^a, Feiyi Wang^{a,*}

^a Hubei Collaborative Innovation Center for Advanced Organic Chemical Materials & Ministry of Education Key Laboratory for the Synthesis and Application of Organic Functional Molecules & State Key Laboratory of Biocatalysis and Enzyme Engineering, Hubei University, Wuhan 430062, China

^b Key Laboratory for Green Chemical Process of Ministry of Education and School of Chemistry and Environmental Engineering, Wuhan Institute of Technology, Wuhan 430205, China

ARTICLE INFO

Article history:

Received 5 November 2020

Received in revised form 28 December 2020

Accepted 29 December 2020

Available online 5 January 2021

Keywords:

Fast-response

Fluorescent probe

Tyrosinase

Good biocompatibility

Fluorescence imaging

ABSTRACT

Tyrosinase (TYR) is an important polyphenolic oxidase enzyme and usually regards as a biomarker of melanoma cancer. Highly effective tracking TYR activity *in vivo* will help to study the mechanism of TYR in living organisms and forecasts related diseases. In this study, we present a novel TYR-activatable fluorescent probe (CHMC-DOPA) for tracking TYR activity *in vitro* and *in vivo*. CHMC-DOPA is constructed by incorporating dopamine (DOPA) moiety into a fluorescent chloro-hydroxyl-merocyanine (CHMC) scaffold. Upon exposure to TYR, the dopamine unit in CHMC-DOPA is oxidized to a dopaquinone derivative, and an intramolecular photo-induced electron transfer (PET) process between CHMC fluorophore and *o*-dopaquinone will take place, the fluorescence of CHMC-DOPA is quenched rapidly. Therefore, the evaluation of TYR activity is established in terms of the relationship between fluorescence quenching efficiency and TYR activity. In our experiments, CHMC-DOPA shows various advantages, such as fast response (8 min), low concentration of TYR activation (0.5 U/mL), good water-solubility, as well as the lowest detection limit (0.003 U/mL) compared with previously reported works. Furthermore, CHMC-DOPA also exhibits excellent cell membrane permeability and low cytotoxicity, which is successfully used to monitor endogenous TYR activity in living cancer cells and zebrafish models. CHMC-DOPA performs well, and we anticipate that this newly designed novel platform will provide an alternative for high effective monitoring TYR activity in biosystems.

© 2021 Chinese Chemical Society and Institute of Materia Medica, Chinese Academy of Medical Sciences.

Published by Elsevier B.V. All rights reserved.

Enzymes play an essential role in various biological and physiological events, abnormal expression of enzymes is often associated with a disease, especially cancer. Therefore, accurate and real-time monitoring of enzymes in organisms is of great importance [1–3]. Tyrosinase (TYR, EC 1.14.18.1), is a glycosylated and copper-containing polyphenol oxidase, which widely exists in plants, microorganisms, and animals [4]. It can specifically catalyze the hydroxylation of monophenols compounds to *o*-diphenol derivatives and subsequently the oxidation of *o*-diphenol derivatives to the corresponding *o*-quinone products in the presence of molecular oxygen [5]. The performances of TYR in these catalytic processes are

considered to be a key factor in the biosynthetic pathway of melanin, which is associated with several severe skin diseases [6,7]. For example, lower expression of TYR will lead to the deficiency of melanin in human bodies and making people suffer from vitiligo or albinism. The excessive expression of TYR indicated that more melanin will be produced and pigmentation, which probably a dangerous signal for malignant melanoma. Thus, tyrosinase is regarded as a biomarker for melanoma and related diseases. Furthermore, several kinds of research have shown that TYR is also associated with the diseases of the immune system and nervous system, which are responsible for schizophrenia and Parkinson's disease (PD) [8,9]. Therefore, the development of a highly sensitive detection method for trapping TYR activity would be of great importance for both fundamental research and clinical application.

Indeed, several analytical methods have been developed for the detection of TYR activity, such as electrophoresis, electrochemical,

* Corresponding authors.

E-mail addresses: lucf@hubu.edu.cn (C. Lu), qisun@wit.edu.cn (Q. Sun), wangfyi@hubu.edu.cn (F. Wang).

radiometric and colorimetric methods, etc. [10,11]. However, most of them are time-consuming, costly, labor-intensive, and inevitable invasion, which makes these analytical methods facing various limitations. Fluorescent techniques are powerful tools to track biotargets, offering ultra-sensitivity, excellent spatiotemporal resolution, noninvasive for imaging, and simplicity in operation [12–36]. To date, several fluorescence sensing systems have been developed for real-time monitoring TYR activity *in vitro* and *in vivo* [4,37–51]. However, the majority of available fluorescent probes have shortcomings associate with very long reaction time (> 180 min), activated with quite high TYR concentrations (> 200 U/mL), unsatisfied detection limit, and poor water-solubility [38,45,46,49,50]. *In situ* tracking of endogenous TYR activity is still handicapped by a lack of novel platform with highly effective. To address these issues, a new fluorescent platform that could overcome the aforementioned disadvantages is urgently demanded.

Herein, we describe the synthesis and biological evaluations of a novel fluorescent probe (CHMC-DOPA) for high effective detection of TYR *in vitro* and *in vivo*. CHMC-DOPA is constructed by using a NIR-emitting fluorophore (CHMC) which contains a semi-cyanine salt unit as the fluorescence reporter, and dopamine (3,4-dihydroxy phenylethylamine, DOPA) with free amino function covalently attached to the CHMC scaffold as the triggered moiety. Upon exposure to TYR, in the presence of molecular oxygen, dopamine moiety in CHMC-DOPA can be rapidly oxidized to *o*-dopaquinone, which then acted as an effective electron acceptor in this platform. Meanwhile, the intramolecular electron transfer from CHMC fluorophore to *o*-dopaquinone in this novel system could take place, and the fluorescence of this conjugate is quenched at the same time due to the PET process (Scheme 1). In this way, the accurate evaluation of TYR activity can be established on the correlation between fluorescence signal output and present TYR activity [49]. In later experiments, as expected, CHMC-DOPA realized the highly effective detection of TYR in the near-infrared region. It should be noted that CHMC-DOPA performs outstanding advantages: (i) CHMC-DOPA exhibits fast response (8 min), low TYR activation (0.5 U/mL), as well as the lowest detection limit (0.003 U/mL) compared with previously reported works (Table S1 in Supporting information). (ii) CHMC-DOPA shows good water solubility, excellent cell membrane permeability, and low cytotoxicity, which is successfully used to track endogenous LAP activity in living cancer cells and zebrafish models. This developed novel sensing system was facile, time-saving, more sensitive, making CHMC-DOPA an alternative method for monitoring TYR activity *in vitro* and *in vivo* with high effective.

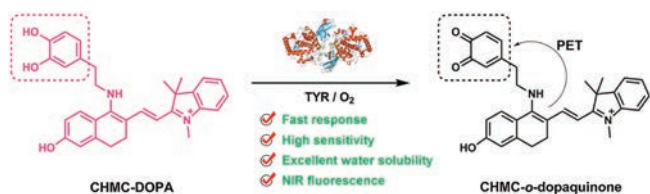
In our probe design, hydrophilicity and NIR emission are considered as the key point. Water solubility is the precondition for biological application and the NIR fluorescence signal can dramatically eliminate the interference from auto-fluorescence from the samples. With these in mind, a new fluorescent probe (CHMC-DOPA) was designed and synthesized. By incorporating a dopamine (DOPA) unit as the trigger moiety into a fluorescent chloro-hydroxyl-merocyanine (CHMC) scaffold [52], a novel fluorescent probe CHMC-DOPA is constructed. In our probe, the

semi-cyanine salt unit can not only significantly improve the water solubility but also endows CHMC-DOPA a typical feature of cyanine dyes, which extends the emission wavelength to the near-infrared (NIR) region.

CHMC-DOPA was synthesized as outlined in Scheme S1 (Supporting information). CHMC smoothly reacted with dopamine through nucleophilic substitution to offer the probe. The chemical structure was well characterized by ¹H and ¹³C NMR spectroscopy and high-resolution mass spectrometry (HRMS) (Fig. S1 in Supporting information).

At the first step, the photophysical properties of CHMC-DOPA towards TYR were initially explored in phosphate-buffered saline (PBS) aqueous solution. Under physiological conditions (PBS buffer solution, 20 mmol/L, pH 7.4, 37 °C), as exhibited in Figs. 1a and b, free CHMC-DOPA showed a sharp absorption band with a peak at 538 nm ($\epsilon = 1.45 \times 10^4 \text{ L mol}^{-1} \text{ cm}^{-1}$) and a strong emission band at 629 nm ($\Phi_F = 0.0395$). Upon incubation with TYR (0.5 U/mL), the absorption and fluorescence spectra of CHMC-DOPA (10 $\mu\text{mol/L}$) showed time-dependent features. UV absorption at $\lambda_{\text{ab}} = 538 \text{ nm}$ decreased expeditiously and a concomitant appearance of a new absorption band at 377 nm was observed. In the fluorescence spectra, the strong emission band of CHMC-DOPA at 629 nm rapidly quenched by TYR in 8 min, which makes it possible to rapid detection of TYR with fluorescence. Moreover, when we try to use a higher level of TYR, such as 1 U/mL, the fluorescence can be quenched within 4 min (Fig. S2 in Supporting information). The response time was much shorter than previously reported works, indicative of the rapid activation of CHMC-DOPA by TYR. However, this intensive and rapid fluorescence signal change could be significantly suppressed by kojic acid (a broad-spectrum inhibitor of tyrosinase) in a dose-dependent manner. As illustrated in Fig. S3 (Supporting information), kojic acid has little influence on the fluorescence of CHMC-DOPA. While in the presence of TYR, with the concentrations of kojic acid increased, the fluorescence response of CHMC-DOPA to TYR was found to be gradually inhibited, indicating that the fluorescence signal change is specific induced by TYR activity. These dramatic fluorescent responses could be ascribed to the oxidation of catechol moiety to *o*-quinone in CHMC-DOPA to arouse the PET effect.

To further evaluate the ability of TYR catalysis of CHMC-DOPA to *o*-dopaquinone derivative, the titration experiments of the enzyme-catalyzed reaction between TYR and CHMC-DOPA was explored in the assay. As exhibited in Fig. 1c, with the increasing concentration of TYR (0–0.5 U/mL) incubated with CHMC-DOPA (10 $\mu\text{mol/L}$) under physiological conditions, the fluorescence intensity decreased gradually and a good linear relationship was observed (inset of Fig. 1c), which makes it possible for quantitative and precise measurements of TYR activity. The detection limit was then determined to be 0.003 U/mL for TYR ($3\sigma/k$), which is much lower than previously reported works. Moreover, the response rate of CHMC-DOPA to TYR was evaluated by time-course fluorescence intensity measurement. In the presence of TYR, the fluorescence intensity of CHMC-DOPA solution gradually decreased and reached a minimum level at about 8 min (Fig. 1d), indicative of the rapid detection of TYR. Meanwhile, without TYR, free CHMC-DOPA shows almost no fluorescence change under the same physiological conditions, demonstrating that the fluorescence variation is triggered by TYR and CHMC-DOPA has good stability for practical applications. Comparatively, CHMC-DOPA performs quite well, it is not only saving much time in detection but also possess a much lower detection limit (Table S1 in Supporting information). To the best of our literature survey, CHMC-DOPA becomes the fastest response fluorescent probe for TYR with the lowest detection limit. Obviously, the high feedback to TYR endows CHMC-DOPA to be an excellent fluorescent probe for tracking trace amounts of intracellular TYR.



Scheme 1. Proposed sensing mechanism for TYR enzymatic activation of CHMC-DOPA.

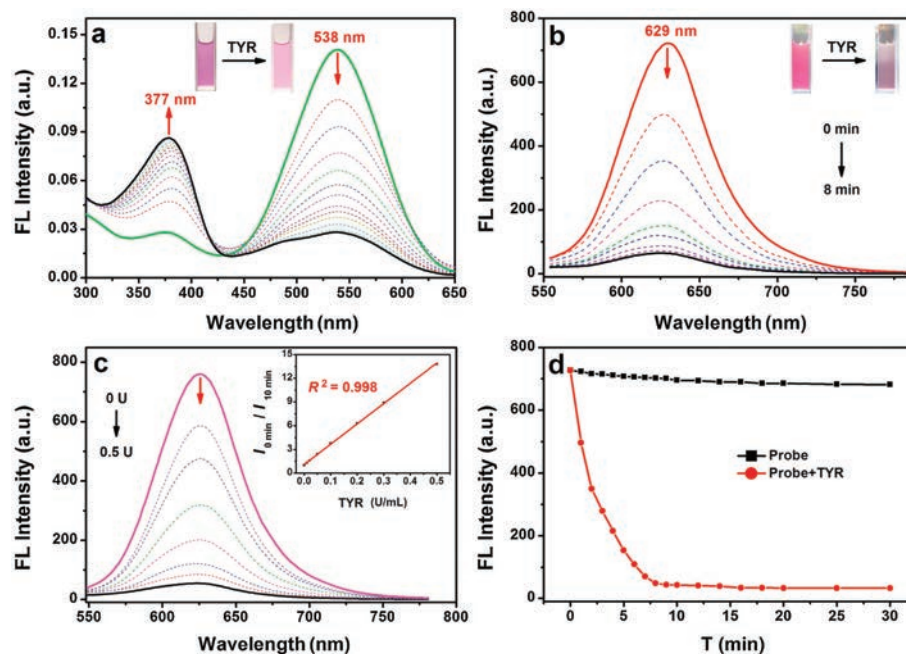


Fig. 1. Time-dependent (a) UV-vis absorption and (b) fluorescence spectra changes of CHMC-Dopa (10 $\mu\text{mol/L}$) in the presence of TYR (0.5 U/mL) in aqueous solution (PBS, 20 mmol/L, pH 7.4) at 37 °C. Inset (a and b): images of CHMC-DOPA solutions before and after treatment with TYR. (c) Emission spectra of CHMC-DOPA (10 $\mu\text{mol/L}$) upon treatment with various concentrations of TYR (0–0.5 U/mL) for 10 min. Inset (c): Emission ratio $I_{0 \text{ min}}/I_{10 \text{ min}}$ as a function of LAP concentrations. (d) Fluorescence intensity at 629 nm as a function of time. $\lambda_{\text{ex}} = 530 \text{ nm}$.

To deeply insight into the sensing mechanism behind the fluorescence variation of CHMC-DOPA in the presence of TYR, we subjected the reaction system to LC-MS analysis. As illustrated in Fig. S4 (Supporting information), pure CHMC-DOPA gave a retention time at about 2.980 min. After mixed with TYR for 5 min, the desiring dopaquinone derivative becomes the main product with retention at 2.560 min was clearly observed, and a mass peak at 479.2295 (identical to $[\text{CHMC-}o\text{-dopaquinone}]^+$) was also detected in this reaction system. These results convincingly demonstrated that TYR played an active role in oxidizing the catechol moiety in CHMC-DOPA to corresponding *o*-quinone, and the intramolecular electron transfer from CHMC fluorophore to *o*-quinone is expected to cause the fluorescence quenching of CHMC-DOPA.

Since the probe was designed to detect TYR in biological systems, CHMC-DOPA needs to prove its stability and sensing reliability in complex microenvironments. Thus, we first investigated the fluorescence intensity of CHMC-DOPA in buffer solutions with different pH values and different temperatures with or without TYR. To our delight, the emission of CHMC-DOPA remained stable and exhibited minimal variation in a wide range of pH values and temperatures. Meanwhile, the fluorescence intensity of CHMC-DOPA can be significantly quenched by TYR in the same conditions (Fig. S5 in Supporting information). And then, we evaluated the chemoselectivity of CHMC-DOPA towards a variety of ions, amino acids, enzyme species, and other biomolecules, it is vital to investigate the stability and selectivity of CHMC-DOPA in these conditions. Results were presented in Fig. 2, by measuring the fluorescence ratio value at $I_{0 \text{ min}}/I_{10 \text{ min}}$ in PBS buffer solution, only such a remarkable enhancement ratio response was observed when the addition of 0.5 U TYR, whereas in the presence of other relevant bioanalytics, such as ions (Ca^{2+} , K^+ , Zn^{2+} , Fe^{3+} , Al^{3+} , and HS^-), amino acids (GSH, Cys and Hcy), several other enzymes (aprotinin, cellulase, trypsin, α -amylase, lipase, sulfatase, chymotrypsin, LAP, ELA, β -Gal, α -Chy), and other bioanalytics (glucose), induced no observable fluorescence ratio change. Particularly, CHMC-DOPA was also exposed to oxidizing

agents including OCI^- , NO_2^- and H_2O_2 , negligible fluorescence ratio changes were detected under these conditions. These results reveal that CHMC-DOPA shows the excellent selectivity towards TYR over other bioanalytics including oxidizing agents, this ascribes to the catechol unit as a specific enzyme-active trigger moiety, and CHMC-DOPA holds the potential for monitoring endogenous LAP in living cells.

Inspired by the excellent sensing properties *in vitro*, we next try to evaluate the capability of our probe for tracking endogenous TYR activity in living samples. Firstly, the cytotoxicity of free CHMC-DOPA was systematically investigated using typical MTT assay, the result clearly showed that the viability of the cells was higher than 95% after incubated for 24 h (Fig. S6 in Supporting information), indicative of the low cytotoxicity of CHMC-DOPA to cells.

Considering the good biocompatibility, we next explore the probe performance in HepG2 cells. As can be seen from Fig. 3, after incubation with CHMC-DOPA (10 $\mu\text{mol/L}$) for 20 min, HepG2 cells afforded a bright fluorescence in the red channel (Figs. 3a–c), showing the staining of CHMC-DOPA in cells. However, with the

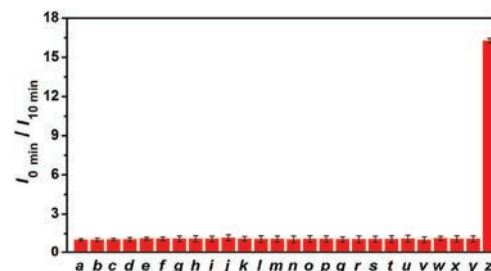


Fig. 2. Fluorescence ratio ($I_{0 \text{ min}}/I_{10 \text{ min}}$) responses of CHMC-DOPA (10 $\mu\text{mol/L}$) in the presence of various analytes. Labels: a: Free; b: Ca^{2+} ; c: K^+ ; d: Zn^{2+} ; e: Fe^{3+} ; f: Al^{3+} ; g: HS^- ; h: OCI^- ; i: NO_2^- ; j: H_2O_2 ; k: GSH; l: Cys; m: Hcy; n: aprotinin; o: cellulase; p: trypsin; q: α -amylase; r: lipase; s: sulfatase; t: chymotrypsin; u: LAP; v: ELA; w: β -Gal; x: α -Chy; y: glucose; z: TYR. Fluorescence intensity was determined at 629 nm in PBS buffer solution at 37 °C. Error bars represent standard deviation ($n = 3$). $\lambda_{\text{ex}} = 530 \text{ nm}$.

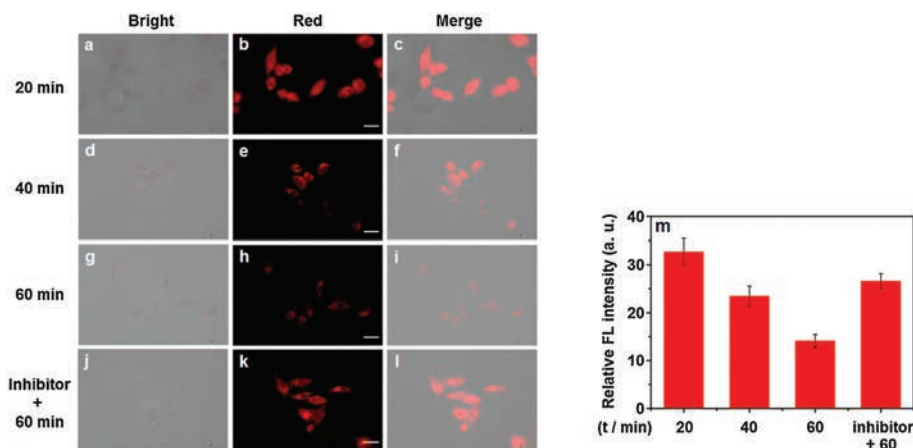


Fig. 3. Visualization of TYR in HepG2 cells by fluorescence microscopy imaging. HepG2 cells incubated with CHMC-DOPA ($10 \mu\text{mol/L}$) for (a–c) 20 min; (d–f) 40 min; (g–i) 60 min. Inhibitor experiments: (j–l) HepG2 cells pretreated with kojic acid ($200 \mu\text{mol/L}$) for 30 min, and then loaded with CHMC-DOPA ($10 \mu\text{mol/L}$) for another 60 min. (a, d, g, j) bright field images; (b, e, h, k) red channel images; (c, f, i, l) merge images. Scale bar = $20 \mu\text{m}$. (m) Average fluorescence intensity. Red channel collected from 590 nm to 650 nm. Error bars represent standard deviation ($n = 3$).

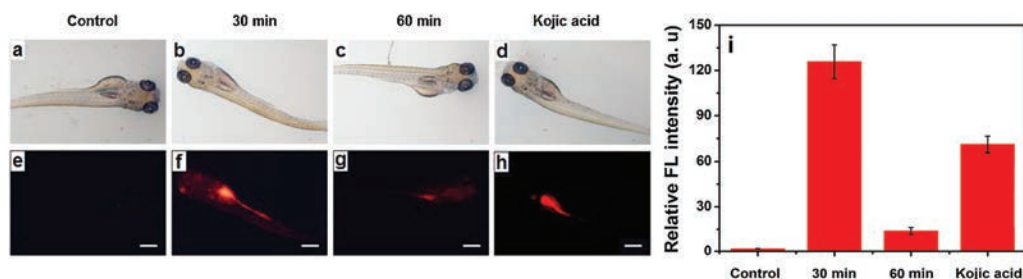


Fig. 4. Fluorescence imaging of zebrafish larvae: (a, e) zebrafish only, (b, f) zebrafish incubated with CHMC-DOPA ($10 \mu\text{mol/L}$) for 30 min; (c, g) zebrafish incubated with $10 \mu\text{mol/L}$ CHMC-DOPA for 60 min; (d, h) zebrafish pretreated with kojic acid ($500 \mu\text{mol/L}$) for 1 h, and then loaded with $10 \mu\text{mol/L}$ CHMC-DOPA for another 60 min. Scale bar = $200 \mu\text{m}$. (i) Average fluorescence intensity. Red channel collected from 590 nm to 650 nm. Error bars represent standard deviation ($n = 3$).

incubation time variation, the fluorescence signal in HepG2 cells gradually declined (Figs. 3d–i), indicating that TYR is overexpressed in HepG2 cells and trigger the fluorescence of CHMC-DOPA quenched, which is consistent well with the optical sensing properties *in vitro*. To further confirm the probe sensing behavior in cancer cells, inhibitor experiments were also conducted. As shown in Figs. 3j–l, the strong NIR fluorescence signal in HepG2 cells was well preserved in the presence of kojic acid, a TYR inhibitor, and the sensing performance between CHMC-DOPA and TYR is blocked. These results demonstrated that these distinct fluorescence signal changes were specifically triggering by intracellular TYR.

To further examine the capability of CHMC-DOPA for tracking TYR activity *in vivo*, we specifically chosen zebrafish for later *in vivo* experiments. According to the previous report [39], tyrosinase is highly expressed in the zebrafish embryonic period, and it will disperse to the whole epidermis as the zebrafish growing up, that is making zebrafish an ideal model. As illustrated in Fig. 4, free zebrafish displayed no background fluorescence in the red channel, while after incubated with CHMC-DOPA for 30 min, a bright fluorescence in the belly was observed, indicating that the probe mainly gathers in the abdomen of zebrafish. With the incubation time extended, the fluorescence signal in the red channel gradually decreased, this phenomenon revealed that CHMC-DOPA was significantly consumed by tyrosinase in zebrafish. To confirm this hypothesis, the inhibitor experiment was also carried out, the zebrafish was first pretreated with kojic acid ($500 \mu\text{mol/L}$) for 60 min, and then incubated with CHMC-DOPA for another 60 min.

As expected, most of the fluorescence in the belly of zebrafish was preserved. All these results demonstrated that CHMC-DOPA is tissue permeable and capable of monitoring TYR in living bodies.

In summary, we have designed and synthesized a TYR-activatable fluorescent probe (CHMC-DOPA) for high effective tracking of TYR activity *in vitro* and *in vivo*. CHMC-DOPA is constructed by incorporating dopamine (DOPA) moiety into a fluorescent CHMC scaffold. Upon interaction with TYR, the catechol unit in CHMC-DOPA is oxidized to *o*-quinone which induces an intramolecular electron transfer from CHMC fluorophore to *o*-dopaquinone, and the fluorescence of CHMC-DOPA is selectively and rapidly quenched, so as to realize the chemoselective detection of TYR. As demonstrated, CHMC-DOPA shows various advantages, such as fast response (8 min), low concentration of TYR activation (0.5 U/mL), good water-solubility, as well as the lowest detection limit (0.003 U/mL). Furthermore, CHMC-DOPA also exhibits excellent cell membrane permeability and low cytotoxicity, which is successfully used to detect TYR activity in living cancer cells and zebrafish models. Consequently, our newly designed fluorescent probe has significantly improved the sensitivity and biocompatibility concerning the previously reported fluorescent probes, thereby providing an alternative for high effective detecting TYR in biosystems.

Declaration of competing interest

The authors report no declarations of interest.

Acknowledgments

We gratefully acknowledge the financial support by the National Natural Science Foundation of China (Nos. 21702053, 21901066, 21676075, 51603064), Natural Science Foundation of Hubei Province (No. 2020CFB601), Outstanding Young and Middle-aged Scientific Innovation Team of Colleges and Universities of Hubei Province (No. T201908), and partially supported by Open Funding Project of the State Key Laboratory of Biocatalysis and Enzyme Engineering.

Appendix A. Supplementary data

Supplementary material related to this article can be found, in the online version, at doi:<https://doi.org/10.1016/j.cclet.2020.12.053>.

References

- [1] J. Zhang, X. Chai, X.P. He, et al., *Chem. Soc. Rev.* 48 (2019) 683–722.
- [2] P. Gao, W. Pan, N. Li, et al., *Chem. Sci.* 10 (2019) 6035–6071.
- [3] K. Gu, Y. Xu, H. Li, et al., *J. Am. Chem. Soc.* 138 (2016) 5334–5340.
- [4] Y. Chen, *Anal. Biochem.* 594 (2020) 113614.
- [5] A. Corani, A. Huijser, T. Gustavsson, et al., *J. Am. Chem. Soc.* 136 (2014) 11626–11635.
- [6] S.A. Shah, N. Raheem, S. Daud, et al., *Clin. Exp. Dermatol.* 40 (2015) 774–780.
- [7] V. Gray-Schopfer, C. Wellbrock, R. Marais, *Nature* 445 (2007) 851–857.
- [8] Y. Teng, X. Jia, J. Li, et al., *Anal. Chem.* 87 (2015) 4897–4902.
- [9] T. Hasegawa, *Int. J. Mol. Sci.* 11 (2010) 1082–1089.
- [10] H.B. Yildiz, R. Freeman, R. Gill, et al., *Anal. Chem.* 80 (2008) 2811–2816.
- [11] R. Freeman, J. Elbaz, R. Gill, et al., *Chem. Eur. J.* 13 (2007) 7288–7293.
- [12] J. Cao, W. Sun, J. Fan, *Chin. Chem. Lett.* 31 (2020) 1402–1405.
- [13] Y. Huang, Y. Zhang, F. Huo, et al., *J. Am. Chem. Soc.* 142 (2020) 18706–18714.
- [14] W.T. Dou, Z.Y. Qin, J. Li, et al., *Sci. Bull.* 64 (2019) 1902–1909.
- [15] J. Han, X. Yue, J. Wang, et al., *Chin. Chem. Lett.* 31 (2020) 1508–1510.
- [16] Y. Fang, J. Shang, D. Liu, et al., *J. Am. Chem. Soc.* 142 (2020) 15271–15275.
- [17] F. Wang, Y. Zhu, L. Zhou, et al., *Angew. Chem. Int. Ed.* 54 (2015) 7349–7353.
- [18] F. Wang, L. Zhou, C. Zhao, et al., *Chem. Sci.* 6 (2015) 2584–2589.
- [19] K. Wang, Q. Kong, X. Chen, et al., *Chin. Chem. Lett.* 31 (2020) 1087–1090.
- [20] F. Wang, S. Hu, Q. Sun, et al., *ACS Appl. Bio Mater.* 2 (2019) 4904–4910.
- [21] T. Wang, Q. Sun, H. Xiong, et al., *Sens. Actuators B Chem.* 321 (2020) 128631.
- [22] Y. Yan, X. Zhang, X. Zhang, et al., *Chin. Chem. Lett.* 31 (2020) 1091–1094.
- [23] S. Yuan, F. Wang, G. Yang, et al., *Anal. Chem.* 90 (2018) 3914–3919.
- [24] Z. Guo, Y. Ma, Y. Liu, et al., *Sci. China Chem.* 61 (2018) 1293–1300.
- [25] J. Zhang, Q. Wang, Z. Guo, et al., *Adv. Funct. Mater.* 29 (2019) 1808153.
- [26] X. Luo, H. Yang, H. Wang, et al., *Anal. Chem.* 90 (2018) 5803–5809.
- [27] R. Wang, X. Gu, Q. Li, et al., *J. Am. Chem. Soc.* 142 (2020) 15084–15090.
- [28] J.A. Chen, W. Guo, Z. Wang, et al., *Anal. Chem.* 92 (2020) 12613–12621.
- [29] Q. Fang, L. Yang, H. Xiong, et al., *Chin. Chem. Lett.* 31 (2020) 129–132.
- [30] Y. Yang, C. Zhang, R. Pan, et al., *Chin. Chem. Lett.* 31 (2020) 125–128.
- [31] F. Deng, L. Liu, Q. Qiao, et al., *Chem. Commun.* 55 (2019) 15045–15048.
- [32] F. Ye, W. Huang, C. Li, et al., *Adv. Therap.* 3 (2020) 2000170.
- [33] Y. Wang, F. Yu, X. Luo, et al., *Chem. Commun.* 56 (2020) 4412–4415.
- [34] X. Luo, J. Li, J. Zhao, et al., *Chin. Chem. Lett.* 30 (2019) 839–846.
- [35] S. Long, Q. Qiao, L. Miao, et al., *Chin. Chem. Lett.* 30 (2019) 573–576.
- [36] Y. Chen, L. Li, W. Chen, et al., *Chin. Chem. Lett.* 30 (2019) 1353–1360.
- [37] S. Yang, J. Jiang, A. Zhou, et al., *Anal. Chem.* 92 (2020) 7194–7199.
- [38] Q. Li, C. Yan, J. Zhang, et al., *Dye. Pigment.* 162 (2019) 802–807.
- [39] C. Zhan, J. Cheng, B. Li, et al., *Anal. Chem.* 90 (2018) 8807–8815.
- [40] S. Li, R. Hu, S. Wang, et al., *Anal. Chem.* 90 (2018) 9296–9300.
- [41] X. Wu, X. Li, H. Li, et al., *Chem. Commun.* 53 (2017) 2443–2446.
- [42] H. Li, W. Liu, F. Zhang, et al., *Anal. Chem.* 90 (2017) 855–858.
- [43] J. Zhou, W. Shi, L. Li, et al., *Anal. Chem.* 88 (2016) 4557–4564.
- [44] X. Wu, L. Li, W. Shi, et al., *Angew. Chem. Int. Ed.* 55 (2016) 14728–14732.
- [45] S.Y. Park, M. Won, J.S. Kim, et al., *Sens. Actuators B: Chem.* 319 (2020) 128306.
- [46] P. Kumar, S. Biswas, A.L. Koner, *New J. Chem.* 44 (2020) 10771–10775.
- [47] F. Zhang, L. Xu, Q. Zhao, et al., *Sens. Actuators B: Chem.* 256 (2018) 1069–1077.
- [48] J.S. Sidhu, A. Singh, N. Garg, et al., *Analyst.* 143 (2018) 4476–4483.
- [49] K.N. Bobba, M. Won, I. Shim, et al., *Chem. Commun.* 53 (2017) 11213–11216.
- [50] Z. Li, Y.F. Wang, X. Zhang, et al., *Sens. Actuators B: Chem.* 242 (2017) 189–194.
- [51] J. Zhang, Z. Li, X. Tian, et al., *Chem. Commun.* 55 (2019) 9463–9466.
- [52] H. Chen, Y. Tang, M. Ren, et al., *Chem. Sci.* 7 (2016) 1896–1903.